CrossMark

Electron Bubbles in Superfluid ^{3}He-A: Exploring the Quasiparticle–Ion Interaction

Oleksii Shevtsov[1] · **J. A. Sauls**[1]

Abstract When an electron is forced into liquid ^{3}He, it forms an "electron bubble", a heavy ion with radius, $R \simeq 1.5$ nm, and mass, $M \simeq 100\,m_3$, where m_3 is the mass of a ^{3}He atom. These negative ions have proven to be powerful local probes of the physical properties of the host quantum fluid, especially the excitation spectra of the superfluid phases. We recently developed a theory for Bogoliubov quasiparticles scattering off electron bubbles embedded in a chiral superfluid that provides a detailed understanding of the spectrum of Weyl Fermions bound to the negative ion, as well as a theory for the forces on moving electron bubbles in superfluid ^{3}He-A (Shevtsov and Sauls in Phys Rev B 94:064511, 2016). This theory is shown to provide quantitative agreement with measurements reported by the RIKEN group (Ikegami et al. in Science 341(6141):59, 2013) for the drag force and anomalous Hall effect of moving electron bubbles in superfluid ^{3}He-A. In this report, we discuss the sensitivity of the forces on the moving ion to the effective interaction between normal-state quasiparticles and the ion. We consider models for the quasiparticle–ion (QP–ion) interaction, including the hard-sphere potential, constrained random-phase-shifts, and interactions with short-range repulsion and intermediate-range attraction. Our results show that the transverse force responsible for the anomalous Hall effect is particularly sensitive to the structure of the QP–ion potential and that strong short-range repulsion, captured by the hard-sphere potential, provides an accurate model for computing the forces acting on the moving electron bubble in superfluid ^{3}He-A.

✉ J. A. Sauls
sauls@northwestern.edu

Oleksii Shevtsov
oleksii.shevtsov@northwestern.edu

1 Department of Physics and Astronomy, Northwestern University, Evanston, IL 60208, USA

1 Introduction

Superfluid ^{3}He-A films are the realization of a chiral topological superfluid [1]. In confined geometries superfluid ^{3}He-A possesses a macroscopic ground-state angular momentum, $L_z = (N/2)\hbar$, where N is the number of ^{3}He atoms in the film. The currents responsible for L_z originate from the spectrum of Weyl Fermions confined on the boundary and reflect the broken time-reversal and mirror symmetries of the chiral A-phase [2–6]. Experimental confirmation of these broken symmetries was demonstrated by the RIKEN group by measuring the forces on electrons moving under the free surface of superfluid ^{3}He-A [7–9]. Electrons submerged in superfluid ^{3}He form a polaron-like state, a negative ion, commonly called an "electron bubble", reflecting its spherically symmetric ground-state wave function [10,11]. Electron bubbles have an effective mass $M \simeq 100\, m_3$, where m_3 is the ^{3}He atomic mass, and are approximately 3 nm in diameter [12]. These mesoscopic objects provide a powerful local probe of the excitation spectrum of the quantum fluid. In particular, by studying the mobility of electron bubbles in ^{3}He-A, Ikegami et al. [7] have demonstrated the chiral nature of this superfluid. Skew scattering of quasiparticles by moving electron bubbles in ^{3}He-A generates a transverse force, and thus an anomalous Hall component in the mobility tensor [13]. An essential ingredient to the theory is the effective potential describing the interaction between quasiparticles and ions. The potential determines the t matrix for the scattering of normal-state quasiparticles by the ion. The corresponding phase shifts for normal-state QP–ion scattering are the key input parameters to the theory for the scattering of Bogoliubov quasiparticles by the ion in the superfluid phase. For temperatures above the superfluid transition, $T_c \simeq 1\,\mathrm{mK} \leq T \lesssim 30\,\mathrm{mK}$, the mobility of the negative ion is independent of temperature [14,15], $\mu_{\mathrm{N}}^{\mathrm{exp}} \simeq 1.7 \times 10^{-6}\,\mathrm{m^2/Vs}$, and determined by the normal-state QP–ion transport cross section, $e/\mu_{\mathrm{N}} = n_3\, p_f\, \sigma_{\mathrm{N}}^{\mathrm{tr}}$, where $p_f = \hbar k_f$ is the Fermi momentum, $n_3 = k_f^3/3\pi^2$ is the ^{3}He particle density, and $\sigma_{\mathrm{N}}^{\mathrm{tr}}$ is given by Eq. (8) of Ref. [13]. This relation is used to constrain models for the QP–ion potential.

We discuss sensitivity of the forces on details of the QP–ion potential. For the electron bubble, the simplest model of a hard-sphere potential provides a good description of both the longitudinal and transverse forces on the bubble in chiral superlfuid ^{3}He-A [13]. For repulsive, short-range interactions the details of the QP–ion potential are shown to be relatively unimportant in determining the longitudinal force on the moving electron bubble provided the normal-state transport cross section accounts for the normal-state mobility. The transverse force is shown to be more sensitive to the structure of the QP–ion potential and corresponding phase shifts as a function of the angular momentum channel. QP–ion interactions with intermediate-range attraction, in addition to short-range repulsion, lead to significant discrepancies between theory and experiment for the magnitude and temperature dependence of the transverse force on moving electron bubbles. Only models with strong repulsion at a mesoscopic distance of order the size of the bubble provide good agreement for both the longitudinal

and transverse forces. This explains the success of the single parameter hard-core QP–ion potential in providing quantitative predictions for the forces in the superfluid A-phase.

2 Stokes Drag and the Anomalous Hall Effect of Electrons in ^{3}He-A

Superfluid ^{3}He-A is a condensate of equal-amplitude, spin-aligned Cooper pairs, $\frac{1}{\sqrt{2}}(|\Rightarrow\rangle + |\Leftarrow\rangle)$, each with an orbital wave function, or mean-field order parameter, $\Delta(\mathbf{p}) = \Delta(\hat{\mathbf{m}} + i\hat{\mathbf{n}}) \cdot \mathbf{p}/p_f$, where $\mathbf{p}$ is the relative momentum of the Cooper pair. Each Cooper pair has orbital angular momentum projection $\hbar$ along the axis $\hat{\mathbf{l}} \equiv \hat{\mathbf{m}} \times \hat{\mathbf{n}}$. The ground state spontaneously breaks time-reversal symmetry (T), parity (P), orbital (SO(3)$_L$) and spin (SO(3)$_S$) rotation symmetries in addition to gauge symmetry (U(1)$_N$). However, these symmetries are only partially broken. The residual symmetry of the A-phase is $H = \text{SO(2)}_{S_z} \times \text{U(1)}_{N\text{-}L_z} \times \text{C}$, where $\text{C} = \text{T} \times \text{P}_m$ is *chiral* symmetry defined as the product of time-reversal and mirror symmetry (P_m) in a plane containing the chiral axis $\hat{\mathbf{l}}$: $\text{P}_m \hat{\mathbf{m}} = +\hat{\mathbf{m}}$, $\text{P}_m \hat{\mathbf{n}} = -\hat{\mathbf{n}}$, and thus $\text{P}_m \hat{\mathbf{l}} = -\hat{\mathbf{l}}$. Similarly, $\text{T}(\hat{\mathbf{m}} + i\hat{\mathbf{n}}) = (\hat{\mathbf{m}} - i\hat{\mathbf{n}})$, and thus $\text{T} \hat{\mathbf{l}} = -\hat{\mathbf{l}}$, i.e. both time-reversal and mirror symmetry are broken in ^{3}He-A, but chiral symmetry, $\text{C} = \text{T} \times \text{P}_m$, is preserved. For our purposes the other important residual symmetry of ^{3}He-A is rotational symmetry about the chiral axis *modulo* a gauge transformation, i.e. the group U(1)$_{N\text{-}L_z}$. Thus, observables such as the superfluid density that are described by a rank two tensor are constrained to be uniaxial. In particular the force on an electron bubble moving with velocity $\mathbf{v}$ in superfluid ^{3}He-A,

$$\mathbf{F}_{\text{QP}} = -\overset{\leftrightarrow}{\eta} \cdot \mathbf{v}, \tag{1}$$

is defined, in the linear response limit, by a Stokes tensor of the form [13],

$$\eta_{ij} = \eta_\perp \left(\delta_{ij} - \hat{l}_i \hat{l}_j\right) + \eta_\parallel \hat{l}_i \hat{l}_j + \eta_{\text{AH}} \epsilon_{ijk} \hat{l}_k, \tag{2}$$

where ϵ_{ijk} is the Levi-Civita tensor, and all components of the Stokes tensor are real with $\eta_\perp$ ($\eta_\parallel$) defining the drag force for motion perpendicular (parallel) to the chiral axis. The off-diagonal term, η_{AH}, in the Stokes tensor gives rise to a *transverse* force acting on the ion for motion perpendicular to $\mathbf{l}$. The transverse component of the force is allowed by chiral symmetry, but would vanish if ^{3}He-A were mirror symmetric [13].

Under the action of a uniform electric field, $\mathbf{E} \perp \hat{\mathbf{l}}$, the equation of motion for an electron bubble in ^{3}He-A is

$$M\frac{d\mathbf{v}}{dt} = e\mathbf{E} - \eta_\perp \mathbf{v} - \eta_{\text{AH}}\mathbf{v} \times \hat{\mathbf{l}}. \tag{3}$$

The electric field accelerates the electron bubble, which is opposed by the Stokes drag, $-\eta_\perp \mathbf{v}$, and the transverse force, $-\eta_{\text{AH}}\mathbf{v} \times \hat{\mathbf{l}}$. The latter gives rise to an *anomalous* Hall

effect, characterized by an effective magnetic field,

$$\mathbf{B}_{\text{eff}} = -\frac{c}{e}\eta_{\text{AH}}\,\hat{\mathbf{l}}. \tag{4}$$

The steady-state solution for the terminal velocity is given by $0 = e\mathbf{E} - \overset{\leftrightarrow}{\eta} \cdot \mathbf{v}$, which can be inverted to give,

$$\mathbf{v} = \overset{\leftrightarrow}{\mu} \cdot \mathbf{E}, \tag{5}$$

where the mobility tensor is given by

$$\overset{\leftrightarrow}{\mu} = e\,\overset{\leftrightarrow}{\eta}{}^{-1}, \tag{6}$$

and has the same uniaxial structure as the Stokes tensor in Eq. (2) with $\mu_{\parallel} = e/\eta_{\parallel}$, $\mu_{\perp} = e\,\eta_{\perp}/(\eta_{\perp}^2 + \eta_{\text{AH}}^2)$, and $\mu_{\text{AH}} = -e\,\eta_{\text{AH}}/(\eta_{\perp}^2 + \eta_{\text{AH}}^2)$. For $\mathbf{E} = \mathscr{E}\hat{\mathbf{x}} \perp \hat{\mathbf{l}} \parallel \hat{\mathbf{z}}$ the anomalous Hall angle is given by the ratio of the transverse and longitudinal velocities,

$$\tan\alpha = \frac{v_y}{v_x} = \frac{\eta_{\text{AH}}}{\eta_{\perp}}. \tag{7}$$

The experimental observation of the anomalous Hall effect for electron bubbles moving in ^{3}He-A, including the reversal of the Hall current under $\hat{\mathbf{l}} \to -\hat{\mathbf{l}}$, provided the direct signature of chirality and broken mirror symmetry in ^{3}He-A [7]. The magnitude of the effect is also remarkable, corresponding to an effective magnetic field of order $B_{\text{eff}} \simeq 10^3 - 10^4$ Tesla.

For temperatures $0 < T < T_c$ the microscopic origin of both the drag force and transverse force on the moving electron bubble in ^{3}He-A is multiple scattering of thermally excited Bogoliubov quasiparticles by the quasiparticle–ion potential, combined with branch conversion scattering by the chiral order parameter of ^{3}He-A. The formulation of the scattering theory is described in detail in Ref. [13], and calculations of the structure of the electron bubble embedded in ^{3}He-A, as well as the Stokes tensor, are reported for the hard-sphere model for the QP–ion potential with radius $R = 1.42$ nm ($k_f R = 11.27$), and shown to be in good agreement with the experimental results for the drag and transverse forces reported by the RIKEN group [7,9] for electron bubbles moving in ^{3}He-A. In what follows we discuss the sensitivity of the theoretical predictions to the QP–ion potential. We report theoretical results for the drag and transverse forces for a wide range of models for the QP–ion potential and compare them with the experiments, and the one-parameter hard-sphere potential.

2.1 Normal-State t Matrix

Our theoretical description for the bound-state spectrum and transport properties of an electron embedded in ^{3}He starts with a model for the *effective* interaction, $U(r)$, between a quasiparticle and the ion, which we assume to be short-ranged and isotropic. At short range, the potential is expected to be of order 1 eV based on the energy required to form the electron bubble, while the range of the potential is to be of order

the classical estimate of the electron bubble radius, $R \sim 2$ nm. Thus, the theory for scattering and the transport properties of the ion is in the strong scattering limit for a mesoscopic object and requires a calculation of the full normal-state scattering t matrix. An important observation is that the scattering of quasiparticles can be treated in the elastic limit. The heavy mass of the electron bubble, combined with the QP–ion collision frequency, implies that recoil of the ion is negligible, i.e. QP–ion scattering in normal ^{3}He is to a good approximation elastic [16,17]. In fact for the electric fields employed in the RIKEN experiments, the recoilless limit can be shown to hold down to temperatures of order $T_r \simeq 200\,\mu$K.

At the atomic level the t matrix takes into account multiple scattering of ^{3}He atoms by the potential representing their interaction with the ion, and is given by a solution of the Lippmann–Schwinger equation [18],

$$T^R = V + VG^R T^R, \tag{8}$$

where G^R is the causal propagator for ^{3}He Fermions.

At low temperatures, $k_B T \ll E_f$, only quasiparticle excitations with momenta near the Fermi surface, $\mathbf{k} \simeq k_f \hat{\mathbf{k}}$, determine the transport and thermodynamic properties of ^{3}He liquid. The corresponding excitation energies, $\xi_{\mathbf{k}} = \hbar v_f(|\mathbf{k}| - k_f)$, satisfy $|\xi_{\mathbf{k}}| \ll E_f$. In the low-energy limit, the equation for the t matrix is obtained by isolating the quasiparticle pole term, $G^R_{\text{low}} \sim (E + i0^+ - \xi_{\mathbf{k}})^{-1}$, in the full propagator, $G^R = G^R_{\text{low}} + G^R_{\text{high}}$. The high-energy propagator renormalizes V to the QP–ion effective interaction, $U = V + VG^R_{\text{high}}U$. This is the interaction determining the scattering of low-energy quasiparticles by the electron bubble in normal ^{3}He. The resulting equation for the QP–ion t matrix, $t^R_N(\hat{\mathbf{k}}', \hat{\mathbf{k}}; E) \equiv \langle \mathbf{k}'|T^R|\mathbf{k}\rangle$, describing elastic scattering of quasiparticles with energy $|E| \ll E_f$ between states with initial $\mathbf{k} = k_f\hat{\mathbf{k}}$ and final $\mathbf{k}' = k_f\hat{\mathbf{k}}'$ momenta is

$$t^R_N(\hat{\mathbf{k}}', \hat{\mathbf{k}}; E) = u(\hat{\mathbf{k}}', \hat{\mathbf{k}}) + \int \frac{d\Omega_{\mathbf{k}''}}{4\pi} u(\hat{\mathbf{k}}', \hat{\mathbf{k}}'')\, g_N(\hat{\mathbf{k}}'', E)\, t^R_N(\hat{\mathbf{k}}'', \hat{\mathbf{k}}; E), \tag{9}$$

where integration is performed over the directions of the intermediate momentum $\mathbf{k}'' = k_f\hat{\mathbf{k}}''$. Here, $g_N(\hat{\mathbf{k}}'', E) = N_f \int d\xi_{\mathbf{k}''}\, G^R_{\text{low}}(\mathbf{k}'', E) = -i\pi N_f$ is the ξ-integrated quasiparticle propagator, $N_f = m^* k_f / 2\pi^2\hbar^2$ is the single-spin density of states at the Fermi surface, and $m^* = p_f/v_f$ is the quasiparticle effective mass. The matrix elements of the effective potential, $u(\hat{\mathbf{k}}', \hat{\mathbf{k}}) = \langle \mathbf{k}'|U|\mathbf{k}\rangle$, as well as the t matrix, are evaluated on the Fermi surface.

The effective potential is assumed to be spherically symmetric for the ground-state of the electron bubble [11]. Thus, we use standard partial-wave analysis to represent the t matrix in terms of partial-wave amplitudes and Legendre polynomials,

$$u(\hat{\mathbf{k}}', \hat{\mathbf{k}}) = \sum_{l=0}^{\infty}(2l + 1)u_l P_l(\hat{\mathbf{k}}' \cdot \hat{\mathbf{k}}), \tag{10}$$

$$t_N^R(\hat{\mathbf{k}}', \hat{\mathbf{k}}; E) = \sum_{l=0}^{\infty} (2l + 1) t_l^R(E) P_l(\hat{\mathbf{k}}' \cdot \hat{\mathbf{k}}). \tag{11}$$

Equation (9) is then solved in terms of the t-matrix amplitudes, $t_l^R(E) = u_l/(1 + i\pi N_f u_l)$, which are parameterized in terms of the scattering phase shift for each angular momentum channel, $\delta_l = -\tan^{-1}\left(\pi N_f u_l\right)$,

$$t_l^R(E) = -\frac{1}{\pi N_f} e^{i\delta_l} \sin \delta_l. \tag{12}$$

Note that the structure of the QP–ion potential is encoded in the set of scattering phase shifts. The resulting t matrix determines the differential cross section for QP–ion scattering, and thus the corresponding total and transport cross sections,

$$\frac{d\sigma}{d\Omega_{\mathbf{k}'}} = \left(\frac{m^*}{2\pi\hbar^2}\right)^2 |t_N^R(\hat{\mathbf{k}}', \hat{\mathbf{k}}; E)|^2, \tag{13}$$

$$\sigma_N^{tot} = \int d\Omega_{\mathbf{k}'} \frac{d\sigma}{d\Omega_{\mathbf{k}'}} = \frac{4\pi}{k_f^2} \sum_{l=0}^{\infty} (2l + 1) \sin^2 \delta_l, \tag{14}$$

$$\sigma_N^{tr} = \int d\Omega_{\mathbf{k}'} (1 - \hat{\mathbf{k}} \cdot \hat{\mathbf{k}}') \frac{d\sigma}{d\Omega_{\mathbf{k}'}} = \frac{4\pi}{k_f^2} \sum_{l=0}^{\infty} (l + 1) \sin^2(\delta_{l+1} - \delta_l). \tag{15}$$

The transport cross section determines the normal-state mobility, $\mu_N = e/n_3 p_f \sigma_N^{tr}$, where $p_f = \hbar k_f$ and n_3 is the ^{3}He particle density.

2.2 Scattering Theory for the Superfluid State

The structure and transport properties of electron bubbles in ^{3}He are modified dramatically by the formation of a condensate of bound Cooper pairs. Spontaneous symmetry breaking—particularly broken gauge, parity and time-reversal in ^{3}He-A—has a profound effect on the spectral properties of the electron bubble, as well as the cross section for Bogoliubov quasiparticles scattering off the negative ion. Bogoliubov quasiparticles, which are coherent superpositions of normal-state particles and holes, undergo branch conversion (Andreev) scattering by the chiral order parameter in combination with scattering by the QP–ion potential. Multiple Andreev and QP–ion scattering in ^{3}He-A leads to the formation of a bound spectrum of chiral (Weyl) Fermions, which hybridize with the continuum of nodal quasiparticles to form low-energy resonances with spectral weight confined near the electron bubble [13]. This discrete spectrum of chiral Fermions evolves into a continuous branch of chiral edge states in the limit $R \to \infty$ and is a finite-size realization of the spectrum of Weyl Fermions for the 2D topological phase of ^{3}He-A [2–6].

Branch conversion scattering by the QP–ion potential and chiral order parameter also leads to skew scattering, and to an anomalous Hall effect for the motion of electron bubbles in superfluid ^{3}He-A (c.f. [13] and references therein). The t matrix for

normal-state spin-$\frac{1}{2}$ quasiparticles is expanded to a 4×4 Nambu matrix to encode the particle-hole coherence of Bogoliubov quasiparticles, *and* branch conversion scattering between particle-like ($dE_{\mathbf{k}}/dk > 0$) and hole-like ($dE_{\mathbf{k}}/dk < 0$) excitations by the order parameter $\Delta(\mathbf{k})$. The scattering theory and the transport theory for the forces on moving electron bubbles resulting from scattering of Bogoliubov quasiparticles is described in detail in Ref. [13].

The Lippmann–Schwinger equation for the t matrix describing scattering states in superfluid ^{3}He-A can be expressed in terms of the normal-state t matrix (elevated to Nambu space), and the difference between the normal-state and superfluid Nambu propagators,

$$T_{\mathrm{S}} = T_{\mathrm{N}} + T_{\mathrm{N}}(G_{\mathrm{S}}^{R} - G_{\mathrm{N}}^{R})T_{\mathrm{S}}. \qquad (16)$$

This subtraction allows us to use the normal-state t matrix, which we calculate for a range of models for the QP–ion potential, as *input* to the calculation of the t matrix for scattering of Bogoliubov quasiparticles in superfluid ^{3}He.

The basis of scattering states is obtained by solving the Bogoliubov equation with the pair potential defined by the chiral A-phase order parameter $\Delta(\hat{\mathbf{p}}) = \Delta\sigma_x(\mathbf{p}_x + i\mathbf{p}_x)/p_f$, where $\mathbf{p} = -i\hbar\nabla$ is the relative momentum operator, and σ_x is the Pauli matrix in spin space. We denote particle-like and hole-like Bogoliubov quasiparticle spinors by $|\Psi_{1,\mathbf{k}\sigma}(\mathbf{r})\rangle$ and $|\Psi_{2,\mathbf{k}\sigma}(\mathbf{r})\rangle$, respectively. The total rate for QP–ion scattering with momentum change, $\mathbf{k} \to \mathbf{k}'$, is given by Fermi's golden rule, $\Gamma(\mathbf{k}', \mathbf{k}) = (2\pi/\hbar)\,W(\mathbf{k}', \mathbf{k})\delta(E_{\mathbf{k}'} - E_{\mathbf{k}})$, with

$$W(\mathbf{k}', \mathbf{k}) = \frac{1}{2}\sum_{\sigma,\sigma'=\uparrow,\downarrow}\Big[|\langle\Psi_{1,\mathbf{k}'\sigma'}|T_S|\Psi_{1,\mathbf{k}\sigma}\rangle|^2 + |\langle\Psi_{1,\mathbf{k}'\sigma'}|T_S|\Psi_{2,\mathbf{k}\sigma}\rangle|^2$$
$$+ |\langle\Psi_{2,\mathbf{k}'\sigma'}|T_S|\Psi_{1,\mathbf{k}\sigma}\rangle|^2 + |\langle\Psi_{2,\mathbf{k}'\sigma'}|T_S|\Psi_{2,\mathbf{k}\sigma}\rangle|^2\Big]_{E_{\mathbf{k}'}=E_{\mathbf{k}}}, \quad (17)$$

where $E_{\mathbf{k}} = \sqrt{\xi_{\mathbf{k}}^2 + |\Delta(\hat{\mathbf{k}})|^2}$ is the Bogoliubov quasiparticle excitation energy. A key feature of QP–ion scattering in ^{3}He-A is the violation of microscopic reversibility; the rates for QP scattering by ions embedded in superfluid ^{3}He-A corresponding to momentum transfers $\mathbf{k} \to \mathbf{k}'$ and $\mathbf{k}' \to \mathbf{k}$ are not equivalent, i.e. $W(\mathbf{k}', \mathbf{k}) \neq W(\mathbf{k}, \mathbf{k}')$. The violation of the microscopic reversibility is a consequence of broken time-reversal (T) and mirror (P_m) symmetries in the ^{3}He-A [13]. To highlight the importance of the violation of microscopic reversibility on QP–ion scattering, we separate the rate into mirror symmetric (W^+) and anti-symmetric (W^-) components,

$$W(\mathbf{k}', \mathbf{k}) = W^+(\mathbf{k}', \mathbf{k}) + W^-(\mathbf{k}', \mathbf{k}), \quad W^{\pm}(\mathbf{k}', \mathbf{k}) = \frac{1}{2}\big[W(\mathbf{k}', \mathbf{k}) \pm W(\mathbf{k}, \mathbf{k}')\big]. \qquad (18)$$

The mirror symmetric scattering rate determines the drag force on a moving electron bubble, while the mirror anti-symmetric rate is responsible for the transverse force, and thus the anomalous Hall effect for electron bubbles moving in ^{3}He-A. These forces

are defined in terms of the components of the Stokes tensor [13],

$$\eta_{ij} = n_3 p_f \int_0^\infty dE \left(-2\frac{\partial f}{\partial E} \right) \sigma_{ij}(E), \quad \forall i, j \in \{x, y, z\}, \quad (19)$$

where the components of the energy-resolved transport cross section also separate into symmetric and anti-symmetric tensors, $\sigma_{ij}(E) = \sigma_{ij}^{(+)}(E) + \sigma_{ij}^{(-)}(E)$, corresponding to the signatures of $W^\pm(\mathbf{k}', \mathbf{k})$ under $\mathbf{k}' \leftrightarrow \mathbf{k}$,

$$\sigma_{ij}^{(+)}(E) = \frac{3}{4} \int_{E \geq |\Delta(\hat{\mathbf{k}}')|^2} d\Omega_{\mathbf{k}'} \int_{E \geq |\Delta(\hat{\mathbf{k}})|^2} \frac{d\Omega_{\mathbf{k}}}{4\pi} \left[\left(\hat{\mathbf{k}}'_i - \hat{\mathbf{k}}_i \right) \left(\hat{\mathbf{k}}'_j - \hat{\mathbf{k}}_j \right) \right] \frac{d\sigma}{d\Omega_{\mathbf{k}'}}, \quad (20)$$

$$\sigma_{ij}^{(-)}(E) = \frac{3}{4} \int_{E \geq |\Delta(\hat{\mathbf{k}}')|^2} d\Omega_{\mathbf{k}'} \int_{E \geq |\Delta(\hat{\mathbf{k}})|^2} \frac{d\Omega_{\mathbf{k}}}{4\pi} \left[\varepsilon_{ijk} \left(\hat{\mathbf{k}}' \times \hat{\mathbf{k}} \right)_k \right] \frac{d\sigma}{d\Omega_{\mathbf{k}'}} \left[f(E) - \frac{1}{2} \right], \quad (21)$$

$$\frac{d\sigma}{d\Omega_{\mathbf{k}'}}(\hat{\mathbf{k}}', \hat{\mathbf{k}}; E) = \left(\frac{m^*}{2\pi\hbar^2} \right)^2 \frac{E}{\sqrt{E^2 - |\Delta(\hat{\mathbf{k}}')|^2}} W(\mathbf{k}', \mathbf{k}) \frac{E}{\sqrt{E^2 - |\Delta(\hat{\mathbf{k}})|^2}}, \quad (22)$$

where $f(E)$ is the Fermi–Dirac distribution function. Note that only the mirror symmetric (anti-symmetric) component of the scattering rate, W^+ (W^-), contributes to the energy-resolved cross section, $\sigma_{ij}^{(+)}(E)$ [$\sigma_{ij}^{(-)}(E)$]. Furthermore, $\sigma_{ij}^{(+)}(E)$ is a diagonal tensor and determines *only* the longitudinal drag forces on the moving ion, while $\sigma_{ij}^{(-)}(E)$ is an anti-symmetric tensor that determines the transverse force, and thus the anomalous Hall current.

To compute these forces we calculate the rates, $W^\pm(\mathbf{k}', \mathbf{k})$, based on the formulation outlined above and in more detail in Ref. [13]. The key input to the calculation is the QP–ion potential, and in particular the QP–ion phase shifts that define the normal-state t matrix. We discuss several possible models for QP–ion scattering below.

3 Quasiparticle–Ion Scattering: Models and Phase Shifts

Scattering phase shifts are the imprint of the near-field QP–ion interaction, $U(r)$, on far field, asymptotic, free-particle form for the scattering solutions to the Schrödinger equation; $\psi_{lm}(\mathbf{r}) = R_l(r) Y_l^m(\theta, \phi)$, where $Y_l^m(\theta, \phi)$ are spherical harmonics, and the radial wave function satisfies [19]

$$\frac{1}{r^2} \frac{\partial}{\partial r} \left(r^2 \frac{\partial R_l}{\partial r} \right) + \left[k^2 - \mathscr{U}(r) - \frac{l(l+1)}{r^2} \right] R_l = 0, \quad (23)$$

with $k^2 = 2m^*E/\hbar^2$ and $\mathscr{U}(r) = 2m^*U(r)/\hbar^2$. We consider finite-range potentials such that $U(r) \approx 0$ for $r > a$, in which case the radial wave function for $r > a$ is a linear combination of spherical wave solutions,

$$R_l(r) = A \left[\cos \delta_l \, j_l(kr) - \sin \delta_l \, n_l(kr) \right], \quad (24)$$

where $j_l(kr)$ and $n_l(kr)$ are spherical Bessel functions of the first and second kind, respectively, and A is a normalization constant. The phase shift, $\delta_l(k)$, for angular momentum channel l depends on the wave number, k; in the far field, $kr \gg 1$, $R_l(r) \approx A \sin(kr - l\pi/2 + \delta_l)/kr$, i.e. a free QP solution shifted in phase by δ_l as a result of the near-field interaction with the ion. Matching the near and far field solutions and the first derivatives at $r = a$ provides us with a normalization-independent condition for the log-derivative of R_l at $r = a$,

$$\tan \delta_l(k) = \frac{k j_l'(ka) - \gamma_l j_l(ka)}{k n_l'(ka) - \gamma_l n_l(ka)}, \quad \gamma_l \equiv \frac{\mathrm{d} \ln R_l}{\mathrm{d} r}\bigg|_{r=a^-}. \tag{25}$$

Equation (25) can be used directly to obtain the phase shifts provided the near-field solution $R_l(r)$ for $r < a$ can be found explicitly. For short-range potentials for which there is not an analytic solution, we use the *variable-phase* method to calculate the phase shifts [20]. This method is based on a first-order, nonlinear differential equation for a function, $\chi_l(r, k)$,

$$\frac{\partial \chi_l(r, k)}{\partial r} = -kr^2 \mathscr{U}(r) \Big[\cos \chi_l(r) \, j_l(kr) - \sin \chi_l(r) \, n_l(kr) \Big]^2, \tag{26}$$

which is used to obtain the scattering phase shift $\delta_l(k)$. In particular, for $\chi_l(0, k) = 0$, the solution to Eq. (26) represents the phase shift accumulated by the scattered wave at distance r from the ion. The asymptotic value is the phase shift for each l and k: $\delta_l(k) = \lim_{r \to \infty} \chi_l(r, k)$. The variable-phase method based on Eq. (26) is well suited for numerical calculations. We refer the reader to Ref. [20] for more details.

3.1 Hard-Sphere Model

The simplest model with an analytic solution for the phase shifts is the one-parameter hard-sphere model defined by $U(r < R) = \infty$ and $U(r > R) = 0$, where R is the hard-sphere radius. The phase shifts are found by requiring that $R_l(r = R) = 0$, and thus given by the formula, $\tan \delta_l(k) = j_l(kR)/n_l(kR)$ [19]. The hard-sphere model provides a benchmark for comparison with experimental measurements of the forces on moving ions, as well as with more detailed models for the QP–ion interaction. Model A in Table 1 is the hard-sphere potential with radius for the electron bubble in ^{3}He at $P = 0$ bar, i.e. $k_f R = 11.17$, as determined by the normal-state mobility. The theoretical results for the forces on a moving electron bubble in ^{3}He, and the comparison with the experimental data reported in Refs. [7–9] for the mobility of negative ions in normal and superfluid ^{3}He-A, is given in Ref. [13] and summarized in Fig. 1. Panel (a) shows the longitudinal mobility as a function of temperature, which is in perfect agreement with the experimental data over more than two decades for $0.25 \leq T/T_c < 1$. From the inset, note that the number of angular momentum channels contributing substantially to QP–ion scattering is finite and determined by $l_{\max} \leq k_f R$. For $l > k_f R$ the phase shifts decrease rapidly to zero. Panel (b) shows the tangent of the Hall angle as a function of $\Delta(T)/k_B T$ calculated from the ratio of the

Table 1 Quasiparticle–ion potentials $U(r)$

| Label	Potential	Parameters
Model A	Hard sphere	$k_f R = 11.17$
Model B	Repulsive core and attractive well	$U_0 = 100 E_f, U_1 = 10 E_f, k_f R' = 11, R/R' = 0.36$
Model C	Random-phase shifts 1	$l_{max} = 11$
Model D	Random-phase shifts 2	$l_{max} = 11$
Model E	Pöschl–Teller 1	$U_0 = 1.01 E_f, k_f R = 22.15, \alpha = 3 \times 10^{-5}, n = 4$
Model F	Pöschl–Teller 2	$U_0 = 2 E_f, k_f R = 19.28, \alpha = 6 \times 10^{-5}, n = 4$
Model G	Hyperbolic tangent 1	$U_0 = 1.01 E_f, k_f R = 14.93, b = 12.47, c = 0.246$
Model H	Hyperbolic tangent 2	$U_0 = 2 E_f, k_f R = 14.18, b = 11.92, c = 0.226$
Model I	Soft sphere 1	$U_0 = 1.01 E_f, k_f R = 12.48$
Model J	Soft sphere 2	$U_0 = 2 E_f, k_f R = 11.95$
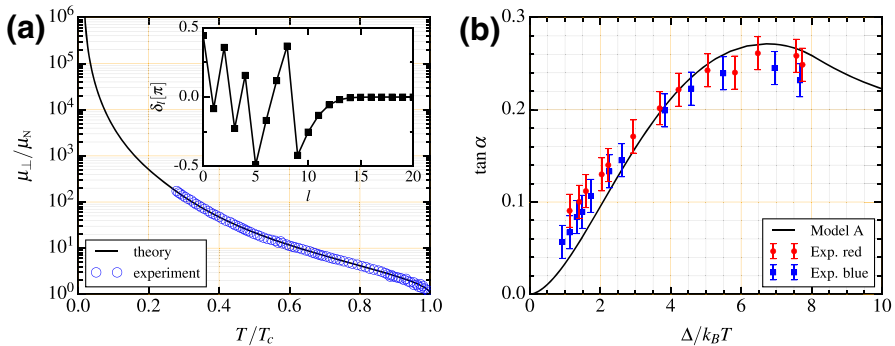
Fig. 1 Comparison of the hard-sphere model (Model A) with data for the mobility of electron bubbles in ^{3}He-A [7,9]. **a** Calculated longitudinal mobility, $\mu_\perp/\mu_N$ versus T/T_c (*black line*), with the *inset* showing the phase shifts for Model A. Experimental data shown as *blue circles*. **b** Calculated anomalous Hall ratio, $\tan \alpha = \eta_{AH}/\eta_\perp$ versus $\Delta(T)/k_B T$ in comparison with data from two different experimental runs (*red* and *blue points*) reported in Refs. [7,9] (Color figure online)

transverse and longitudinal Stokes parameters [Eq. (7)]. The theory based on the hard-sphere model (Model A) is in a good agreement with mobility experiments for electron bubbles, providing confirmation that the microscopic theory for potential and branch conversion scattering of Bogoliubov quasiparticles captures the essential physics and structure of the negative ion moving at low velocity in a chiral superfluid. It is worth noting that the hard-sphere radius R was fixed at the outset by fitting the calculated normal-state mobility to the experimentally measured value and that there are no other adjustable parameters in the calculations for the forces on the ion in superfluid ^{3}He. Nevertheless, it is important to test the robustness of the theoretical predictions by considering a range of models for the QP–ion potential, as well as possible variations in transport properties for ions described by a potential that deviates significantly from that of a hard sphere.

3.2 Piece-Wise Constant Potential with Intermediate-Range Attraction

Among the analytically solvable models, we consider Model B for the QP–ion potential with finite, short-range repulsion and intermediate-range attraction defined by the piece-wise constant potential,

$$U(r) = \begin{cases} U_0, & r < R, \\ -U_1, & R < r < R', \\ 0, & r > R'. \end{cases} \tag{27}$$

Using Eq. (25), we find the following expression for the phase shifts,

$$\tan \delta_l = \frac{(l - \zeta_l) j_l(k_f R') - k_f R' j_{l+1}(k_f R')}{(l - \zeta_l) n_l(k_f R') - k_f R' n_{l+1}(k_f R')}, \quad \zeta_l = x' \frac{a_l}{b_l}. \tag{28}$$

$$a_l = l \left[n_{l+1}(x) j_l(x') - n_l(x') j_{l+1}(x) \right] + x' \left[n_{l+1}(x') j_{l+1}(x) - n_{l+1}(x) j_{l+1}(x') \right]$$

$$+ \frac{l p_l}{x'} \left[n_l(x) j_l(x') - n_l(x') j_l(x) \right] + p_l \left[n_{l+1}(x') j_l(x) - n_l(x) j_{l+1}(x') \right], \tag{29}$$

$$b_l = x' \left[n_{l+1}(x) j_l(x') - n_l(x') j_{l+1}(x) \right] + p_l \left[n_l(x) j_l(x') - n_l(x') j_l(x) \right], \tag{30}$$

with $p_l = z' i_{l+1}(z)/i_l(z)$, $x = \beta_1 k_f R$, $x' = \beta_1 k_f R'$, $z = \beta_0 k_f R$, $z' = \beta_0 k_f R'$, $\beta_0 = \sqrt{(U_0 - E_f)/E_f}$ and $\beta_1 = \sqrt{(U_1 + E_f)/E_f}$, where $i_l(x)$ is the modified spherical Bessel function of the first kind. Note that a purely repulsive soft-core potential case is obtained from Eq. (28) by setting $R = R'$ and $U_1 = 0$, while additionally taking $U_0 \to \infty$ recovers the hard-sphere result.

Model B versus Model A In Fig. 2a, b we compare calculations based on Model A with those based on Model B (parameters are listed in Table 1). Model A is the hard sphere that agrees very well with experiments on the electron bubble in ^{3}He-A. Model B corresponds to strong short-range repulsion, and intermediate-range attraction. The latter allows for a shallow bound state, and therefore a scattering resonance, in one or more high angular momentum channels. In the case of Model B, one can see that there is an *extra* scattering resonance in channel $l = 10$ shown in the inset of Fig. 2a. Figure 2a, b shows that the resonance leads to small deviations of the drag force compared to that for the hard-sphere model (and experiment), but a drastic reduction in the Hall ratio. The basic conclusion is that the electron bubble is well described by strong, short-range repulsion with no intermediate-range attraction. A variant of Model B may be relevant to positive ions, since positive ions attract ^{3}He atoms producing a more complex ionic structure.

3.3 Other QP–Ion Potentials and Scattering Models

Apart from the two exactly solvable models discussed above, we considered several repulsive potentials, as well as a constrained random-phase-shift model (Models C and D in Table 1).
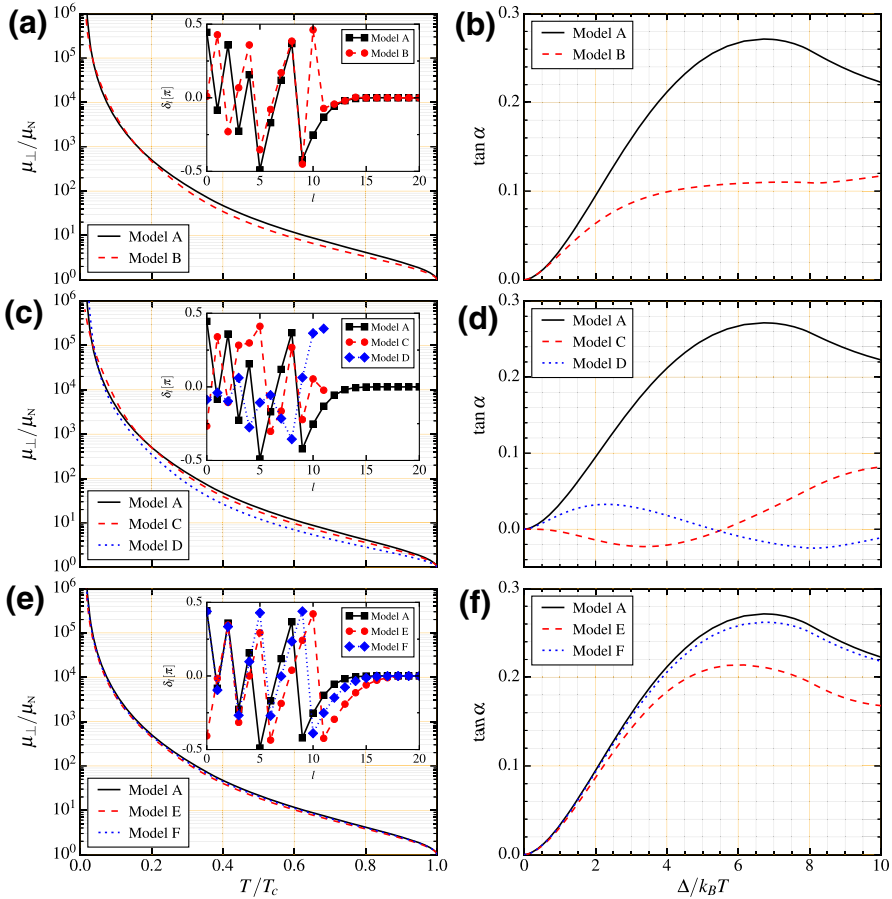
Fig. 2 Comparison of numerical results for longitudinal mobility ($\mu_\perp/\mu_N$) and the Hall ratio ($\tan\alpha = \eta_{AH}/\eta_\perp$) obtained with Models B–F listed in Table 1, in comparison with the hard-sphere model (Model A) (Color figure online)

Models C and D The pattern of phase shifts versus angular momentum for Model A shown in the inset of Fig. 1 is a fingerprint of the hard-sphere QP–ion potential, *with* $k_f R = 11.17$ fixed by the normal-state ion mobility. This constraint fixes the number of relevant scattering channels. Here we consider the sensitivity of forces on the ion to the specific pattern of phase shifts, while keeping the number of scattering channels fixed at $l_{max} = 11$ *and* enforcing the constraint on the transport cross section provided by the normal-state mobility. Models C and D are two different realizations of the *random-phase-shift model* with $l_{max} = 11$, constrained to fit the normal-state ion mobility, μ_N. The procedure is to use a random number generator to calculate $\{\delta_l | l = 1, \ldots, l_{max}\}$, then adjust the phase shift in channel $l = 0$ to satisfy the constraint on the transport cross section. Models C and D differ by the seed used to generate the phase shifts. Note that not every realization of random-phase shifts for $l = 1, \ldots, l_{max}$ allows a fit to experiment by varying the remaining phase shift δ_0. As Fig. 2d shows the

random-phase-shift model fails dramatically to account for the anomalous Hall angle for the electron bubble in ^{3}He-A, and thus the magnitude and temperature dependence of the transverse force on the electron bubble, even though the longitudinal mobility shown in Fig. 2c is relatively close to that of Model A, and therefore to the measured longitudinal force. This basic feature is characteristic of the comparison between theory and mobility measurements for electron bubbles in ^{3}He-A; the longitudinal mobility is relatively insensitive to the QP–ion potential provided the model accounts for the experimental normal-state transport cross section. In contrast, the transverse force is sensitive to the pattern of phase shifts as a function of the angular momentum channel, as well as the transport cross section.

Models E and F Additional motivation for considering a range of models for the QP–ion potential is to see if a refinement to Model A can remove the small deviations between theory and experiment evident in Fig. 1 for the Hall ratio at temperatures near T_c, i.e. for $\Delta(T)/k_B T \rightarrow 0$. Thus, we consider Pöschl–Teller potentials of the form $U(x) = U_0/\cosh^2[\alpha x^n]$, where $x = k_f r$, as well as the hyperbolic tangent model defined by $U(x) = U_0[1 - \tanh[(x - b)/c]]$. In all cases the parameters of the potential are adjusted to fit the normal-state transport cross section to account for the measured normal-state mobility, $\mu_N^{exp} = 1.7 \times 10^{-6}$ m^2/Vs [7].

   In Fig. 2e, f we show numerical results for the Pöschl–Teller model with two different sets of parameters as listed in Table 1. This is a three-parameter model describing a smoothly decaying repulsive potential. As was the case for other models the transverse component of the Stokes tensor, η_{AH}, and thus the Hall angle, is more sensitive to the structure of the potential (Fig. 2f), than is the longitudinal mobility $\mu_\perp$. The phase shifts, particularly those of Model F, are very close to those of Model A (inset of Fig. 2e). The results for Model F are also much closer to Model A, and to experiment, than those of Model E, which is a softer and longer range potential. The general trend is that the numerical results obtained with the Pöschl–Teller potential are almost indistinguishable from Model A in the limit that the strength of the potential is sufficiently repulsive, i.e. $U_0 \gtrsim 6E_f$ (not shown).

Models G, H, I and J Lastly, we consider the hyperbolic tangent and the soft-sphere models, each with two different sets of parameters, indicated in Table 1 as Models G and H and Models I and J, respectively. The numerical results, which are not shown, for these models are barely distinguishable from those of Model A, and in contrast to the Pöschl–Teller model, the results for Models G–J are practically insensitive to variations of the magnitude of the potential U_0, provided $U_0 > E_f$. Finally, we note that the small deviations between theory and experiment for the anomalous Hall ratio persist, suggesting that there may be an additional scattering mechanism not captured by a repulsive, short-range, spin-independent, isotropic QP–ion potential.

4 Conclusions

We considered a number of models for the effective potential describing the interaction between normal-state quasiparticles and ions embedded in ^{3}He. This potential

determines the normal-state scattering phase shifts which are the input parameters to the theory for Bogoliubov quasiparticles scattering off electron bubbles moving in the chiral A-phase of superfluid ^{3}He. We show that the scattering theory developed in Ref. [13], with a strongly repulsive, short-range QP–ion potential—specifically the hard-sphere model—is in very good agreement with experimental measurements of the longitudinal mobility and anomalous Hall current for electron bubbles moving in ^{3}He-A [7–9]. We also show that softer, longer range potentials, as well as potentials with intermediate-range attraction, fail to account for the magnitude and temperature dependence of the Hall angle.

References

1. G.E. Volovik, Sov. Phys. JETP **67**, 1804 (1988)
2. G.E. Volovik, JETP Lett. **55**(6), 368 (1992)
3. M. Stone, R. Roy, Phys. Rev. B **69**(18), 184511 (2004)
4. J.A. Sauls, Phys. Rev. B **84**, 214509 (2011)
5. Y. Tsutsumi, K. Machida, J. Phys. Soc. Jpn. **81**(7), 074607 (2012)
6. Y. Tsutsumi, K. Machida, Phys. Rev. B **85**, 100506 (2012)
7. H. Ikegami, Y. Tsutsumi, K. Kono, Science **341**(6141), 59 (2013)
8. H. Ikegami, S.B. Chung, K. Kono, J. Phys. Soc. Jpn. **82**, 124607 (2013)
9. H. Ikegami, Y. Tsutsumi, K. Kono, J. Phys. Soc. Jpn. **84**(4), 044602 (2015)
10. R.A. Ferrell, Phys. Rev. **108**, 167 (1957)
11. C.G. Kuper, Phys. Rev. **122**, 1007 (1961)
12. A.C. Anderson, M. Kuchnir, J.C. Wheatley, Phys. Rev. **168**, 261 (1968)
13. O. Shevtsov, J.A. Sauls, Phys. Rev. B **94**, 064511 (2016)
14. A.I. Ahonen, J. Kokko, O.V. Lounasmaa, M.A. Paalanen, R.C. Richardson, W. Schoepe, Y. Takano, Phys. Rev. Lett. **37**, 511 (1976)
15. A.I. Ahonen, J. Kokko, M.A. Paalanen, R.C. Richardson, W. Schoepe, Y. Takano, J. Low Temp. Phys. **30**(1), 205 (1978)
16. B.D. Josephson, J. Lekner, Phys. Rev. Lett. **23**, 111 (1969)
17. A.L. Fetter, J. Kurkijärvi, Phys. Rev. B **15**, 4272 (1977)
18. J. Rammer, *Quantum Transport Theory* (Perseus Books, Reading, 1998)
19. A. Messiah, *Quantum Mechanics*, vol. I (North-Holland, Amsterdam, 1958)
20. F. Calogero, *Variable Phase Approach to Potential Scattering* (Academic Press, New York, 1967)